

Determination of $^3J_{\text{HF}}$ and $^4J_{\text{HF}}$ Karplus Relationships for the ϕ and ψ Angles of Peptides Using *N*-Fluoroamides as Models

Charles F. Hammer* and Srinivasan Chandrasegaran†

Contribution from the Department of Chemistry, Georgetown University, Washington, D.C. 20057. Received October 18, 1982

Abstract: A series of *N*-fluoroamide derivatives were synthesized by the reaction of CF_3OF with the corresponding amides. The reaction procedure of Barton et al.¹ was appropriately modified to maximize the yield of the pure monofluoro derivatives. The compounds were examined as models for the determination of the ϕ' ($^3J_{\text{HF}}$) and ψ' ($^4J_{\text{HF}}$) angles of peptides with ^1H , ^{19}F , and ^{13}C NMR spectroscopy. Investigation of this series of compounds has led to Karplus-type relations between ϕ' vs. $^3J_{\text{HF}}$ and ψ' vs. $^4J_{\text{HF}}$ using the experimental coupling constants. As the signs of the coupling constants could not be determined at this time, several possibilities arise for these relations. Of these, the fitted equation ($R = 0.990$), $^3J_{\text{NF-CH}} = 70.8 \cos^2 \phi' - 44.1 \cos \phi' - 7.2$, best describes the angular relation for the ϕ' angle. The fitted equation ($R = 0.983$), $^4J_{\text{NF-CO-CH}} = -19.5 \cos^2 \psi' + 8.8 \cos \psi' + 4.9$, best describes the angular relation for the ψ' angle. The plots of both equations give typical Karplus curves except that they go through zero, i.e., undergo an inversion of sign. Fluorination of the amides causes the chemical shift of the carbonyl carbon to be shifted upfield 4–5 ppm while the carbon α to the nitrogen is shifted downfield 7–12 ppm. Furthermore, these carbons appear as doublets ($^2J_{\text{C-NF}} = 4\text{--}9$ Hz for the $\text{C}=\text{O}$ and $<1.0\text{--}14.7$ Hz for C_α) because of their coupling with the fluorine atom. The ^{19}F chemical shifts of the model *N*-fluoroamide derivatives vary more than 39 ppm (δ_{F} 42 to 81 downfield of external CFCl_3) and are very sensitive to structural changes. It was not possible, however, to observe less than 5-Hz couplings in the ^{19}F spectra because of the quadrupolar broadening caused by the ^{14}N atom.

Introduction

Proteins and peptides are very important for the functioning of organisms. The most striking feature of peptides is that they assume specific spatial conformations essential to their biological activity. In order to define the conformation of a peptide unit, four angles, namely, ϕ , ω , ψ , and χ_1 , must be determined; ϕ , ω , and ψ correspond to the backbone torsion angles while χ_1 relates to the first side-chain torsion angle. While X-ray crystallographic data on the solid-state conformation of many polypeptides have been determined, the solution conformation is frequently different from those found in crystals.^{2,3} One of the most effective methods used to determine solution conformations is NMR spectroscopy. NMR, however, gives a time-averaged spectrum of interconverting low-energy conformations of a polypeptide in solution.

The torsional or rotational angle around the $\text{C}_\alpha\text{H-NH}$ bond is denoted as ϕ' . Vicinal CH-NH proton-proton coupling constants have been used extensively to investigate polypeptide conformations in solution.⁴ This procedure is based on an empirical mathematical relation between the vicinal coupling constant ($^3J_{\text{CH-NH}}$) and the angle ϕ' . This relation is given by a Karplus-type equation (eq 1) similar to one that has been used to

$$^3J_{\text{CH-NH}} = A \cos^2 \phi' + B \cos \phi' + C \quad (1)$$

describe the vicinal coupling constant in the H-C-C-H moiety.⁵ The choice of the parameters A , B , and C depends upon the system under consideration since substituent electronegativities, bond lengths and the dihedral angles, and other molecular properties that affect the spin-spin couplings are not explicit in the equation.⁶ Almost all conformational work on peptides using NMR spectroscopy has been based on this angular dependence of ϕ' , which normally has maxima at $\phi' = 0$ or 180° and a minimum at ca. 85° .⁴ At present, a combination of experimental NMR data ($^3J_{\text{CH-NH}}$ in Hz) and the calculation of potential energy minima appears to be the most popular method of deriving conformational information on peptides.^{7,8} As NMR cannot be used to differentiate between ϕ' and $360^\circ - \phi'$, there usually exist four possible solutions of the angle ϕ' for each experimentally determined 3J . A second determination of ϕ' by a different approach would remove half of the ambiguity provided that the second Karplus relationship is independently obtained and that there has not been any conformational change during the second method.

The torsional angle around the $\text{C}_\alpha\text{-CO}$ bond is designated as ψ , whose determination has eluded researchers until now because the $^4J_{\text{CH-CO-NH}}$ coupling is too small to be observed in ^1H NMR. The use of $\text{H-C}_\alpha\text{-CO-}^{15}\text{N}$ coupling constants to determine ψ has not been successful. Although calculations that predict readily observable magnitudes for $^3J_{\text{H-C-CO-}^{15}\text{N}}$ have been reported,⁹ experimental couplings obtained from actual spectra were too small (<2 Hz) to be useful.¹⁰⁻¹² Since the largest coupling constant (negative) was expected for an $\text{H-C-CO-}^{15}\text{N}$ angle of 180° , Kopple et al.¹³ prepared ^{15}N -enriched 2-azabicyclo[2.2.2]octan-3-one, in which the ψ angle is 180° . By comparing the spectrum of the enriched material with that of the ^{14}N analogue, in which the coupling of the nitrogen is virtually eliminated by its rapid quadrupolar relaxation, Kopple estimated the coupling to be ca. 1.3 Hz. From this, they concluded that the $^3J_{\text{CH-CO-}^{15}\text{N}}$ values are likely to be too small for the determination of the ψ angle and hence in the study of peptide conformations. Ramachandran¹⁴ has developed ϕ vs. ψ maps that are currently used to restrict the possible ψ angles. Clearly an experimental method to determine ψ in solution is badly needed.

In order to determine the angle ψ and to provide a second determination of ϕ' , so as to remove part of the ambiguity in the determination of the latter angle, we have synthesized a series of *N*-fluoroamide derivatives and carefully analyzed their ^1H , ^{13}C , and ^{19}F NMR spectra. The results of this study and the derivation

* Currently at the Johns Hopkins University School of Hygiene and Public Health, Division of Biophysics, Baltimore, MD 21205.

- (1) Barton, D. H. R.; Hesse, Robert H.; Pechet, Maurice M.; Toh, Hee T. *J. Chem. Soc., Perkin Trans. 1* 1974, 732.
- (2) Pease, L. G.; Watson, C. *J. Am. Chem. Soc.* 1978, 100, 1278.
- (3) Karle, I. L. *J. Am. Chem. Soc.* 1978, 100, 1286.
- (4) Bystrov, V. F.; Portnova, S. L.; Balashova, T. A.; Tsetlin, V. I.; Ivanov, V. T.; Kostezky, P. V.; Ovchinnikov, A. *Tetrahedron Lett.* 1968, 5283.
- (5) Scheraga, H. J. *Chem. Phys.* 1959, 30, 11.
- (6) Karplus, H. *J. Am. Chem. Soc.* 1963, 85, 2870.
- (7) Gibbons, W. A.; Nemethy, G.; Stern, A.; Craig, L. C. *Proc. Natl. Acad. Sci. U.S.A.* 1970, 67, 239.
- (8) Scheraga, H. A. *Chem. Rev.* 1971, 71, 195.
- (9) Karplus, S.; Karplus, H. *Proc. Natl. Acad. Sci. U.S.A.* 1972, 69, 3204.
- (10) Sogn, J. A.; Gibbons, W. A.; Randall, E. W. *Biochemistry* 1973, 12, 2100.
- (11) Barfield, M.; Gearhart, H. L. *Mol. Phys.* 1974, 27, 899.
- (12) Bystrov, V. F.; Gavrilov, D.; Solkan, V. N. *J. Magn. Reson.* 1974, 19, 123.
- (13) Kopple, K. D.; Ahsan, A.; Barfield, M. *Tetrahedron Lett.* 1978, 3519.
- (14) Ramachandran, G. N.; Ramakrishnan, C.; Sasikharan, V. *J. Mol. Biol.* 1963, 7, 95.

of the Karplus relations of $^3J_{\text{HF}}$ vs. ϕ' and $^4J_{\text{HF}}$ vs. ψ' are reported in this paper.

Experimental Section

Melting points ($^{\circ}\text{C}$) were measured on a Gallenkamp melting point apparatus and are corrected. Infrared spectra were obtained on neat films (by evaporation of chloroform solutions on a KBr plate) with a Perkin-Elmer Model 457 grating infrared spectrometer. EI mass spectra (direct probe) were obtained on a Finnegan 4000 quadrupole mass spectrometer at 70 eV. NMR spectra were obtained on a Bruker WH/HFX-90 FT-NMR spectrometer equipped with QPD and a 20K BNC-12 Nicolet computer using a deuterium lock and a home-built homonuclear decoupler capable of decoupling a band width of several hundred hertz. The 300.134-MHz ^1H spectra were obtained on a Bruker WN-300 FT-NMR spectrometer kindly loaned by Dr. William Egan of the Bureau of Biologics of the Food and Drug Administration, Washington DC. Me_4Si was used as an internal standard for the ^1H spectra and ^{13}C spectra (22.628 MHz) while CFCl_3 was used as an external standard for the ^{19}F spectra (84.66 MHz). The estimated errors in reported chemical shifts are <0.01 , <0.1 , and <0.2 ppm for ^1H , ^{13}C , and ^{19}F NMR spectra, respectively. The computer resolution of the ^1H coupling constants at 300 MHz are ± 0.18 Hz and at 90 MHz are ± 0.29 Hz. HPLC purifications were performed on a Waters Model 6000A solvent delivery system having a R-601 differential refractometer detection unit. All HPLC solvents (either Alltech or Fisher Scientific) were filtered and degassed before use. All samples were passed through 0.45- μ Millipore filters before injection.

Materials. Deuterated chloroform was obtained from Aldrich Chemical Co. All other solvents for reactions and chromatography were Baker Analyzed reagent grade. Trifluoromethyl hypofluorite (CF_3OF) was obtained from PCR Inc. or kindly synthesized at the Naval Research Laboratory under the direction of Dr. Ronald de Marko. All organic reagents were obtained from Aldrich Chemical Co. except the following: acetic anhydride (J. T. Baker), *N-tert*-butylformamide and stearoyl chloride (Pfaltz and Bauer Co.), and Dowtherm (gift of Dow Chemical Co.).

2-Azabicyclo[2.2.2]octan-3-one (1A) was prepared from *p*-amino benzoic acid according to the procedure of Pearlman:¹⁵ mp 197–198 $^{\circ}$ (lit.¹⁵ 197–198 $^{\circ}$); ^1H NMR (CHCl_3 , 300 MHz) δ 8.1 ppm (NH, bs, 1 H), 3.63 (H_1 , bn, 1 H), 2.48 (H_4 , bm, 1 H), 1.9–1.58 (H_5 , H_6 , H_7 , and H_8 , m, 8 H); ^{13}C NMR (CHCl_3) δ 178.67 ppm (C_3), 47.64 (C_1 , d, 144.1 Hz), 37.89 (C_4 , d, 141.2 Hz), 27.82 (C_5 , C_6 , t, 131.6 Hz), 24.18 (C_6 , C_7 , t, 134.6 Hz); IR (film) 3180 cm^{-1} (amide NH), 2960 (CH), 1680 (amide C=O); EIMS (direct probe) m/e 125 (M^+), 97 ($\text{M}^+ - \text{CO}$), 69 (97 - C_2H_4).

4-Aza-10,10-dimethyltricyclo[5.2.1.0^{1,5}]decan-3-one (2A) was prepared by the reaction of camphene with chlorosulfonyl isocyanate using a slightly modified literature procedure.^{16,17} Hexane was used as the solvent to maximize the yield of **2A**. The intermediate *N*-sulfonyl chloride was reductively hydrolyzed using sodium sulfite in water after removing the hexane on a rotary vaporizer. Recrystallization from water gave white crystals (52% yield): mp 189 $^{\circ}$ (lit.^{16,17} mp 190 $^{\circ}$); ^1H NMR (CDCl_3 , 300 MHz) δ 6.8 ppm (NH, bs, 1 H), 3.492 (H_5 , dd [X of ABX, $J = 8.18$, 4.69 Hz], 2 H), 2.243 and 2.103 (H_{2a} and H_{2b} , AB q [$J = 17.24$ Hz], 2 H), 1.95 (H_{6a} , dm [$J = 12.9$ Hz + ?], 1 H), 1.84 (H_{8a} and H_{9a} , dm [$J = 14.4$ Hz + ?], 2 H), 1.824 (H_7 , m, 1 H), 1.63 (H_{6a} , dd [$J = 12.87$, 8.27 Hz], 1 H), 1.265 (H_{9a} and H_{9a} , dtm [$J = 14.4$, 8.4 Hz], 2 H), 1.00 and 0.908 (H_{11} and H_{12} , 2 s, 3 H each); ^{13}C NMR (CDCl_3) δ 180.37 ppm (C_3), 64.61 (C_5), 54.83 (C_1), 48.13 (C_{10}), 46.41 (C_6), 37.80 (C_7), 34.09 (C_9), 31.88 (C_8), 28.40 (C_2), 21.68 and 21.03 (C_{11} and C_{12}); IR (film) 3205 cm^{-1} (amide NH), 2925 and 2880 (CH), 1700 (amide C=O); EIMS (direct probe) m/e 179 (M^+), 164 ($\text{M}^+ - \text{CH}_3$), 151 ($\text{M}^+ - \text{CO}$), 136 ($\text{M}^+ - \text{HNCO}$).

2-Aza-7,7,8-trimethyltricyclo[4.2.1.0^{4,8}]nonan-3-one (3A) was prepared by the reaction of chlorosulfonyl isocyanate with α -pinene in chloroform according to the procedure of Malpass.¹⁸ The *N*-sulfonyl chloride derivatives, obtained after the removal of the solvent, was hydrolyzed with NaOH in aqueous acetone (pH 6–8) and purified by silica gel column chromatography and HPLC on an ODS column with 15:85 methanol: water (35% yield): mp 205–210 $^{\circ}$ (lit.¹⁸ mp 205–215 $^{\circ}$); ^1H NMR (CDCl_3 , 300 MHz) δ 6.93 ppm (NH, bs, 1 H), 3.373 (H_1 , d [$J = 7.35$ Hz], 1 H), 2.18 (H_4 , bt [$J = 11.35$ Hz], 1 H), 2.06 (H_{5a} and H_{9a} , bd [$J = 10.85$ Hz], 2 H), 1.903 (H_6 , t [$J = 3.77$ Hz], 1 H), 1.563 (H_{9a} , d [J

= 12.69 Hz], 1 H), 1.280 (H_{3a} , d [$J = 13.05$ Hz], 1 H), 1.090 (H_{10} , s, 3 H), 0.931 and 0.922 (H_{11} and H_{12} , 2s, 6 H); ^{13}C NMR (CDCl_3) δ 183.29 ppm (C_3), 60.64 (C_1), 59.15 (C_8), 48.62 (C_7), 48.03 (C_6), 47.51 (C_4), 37.83 (C_5), 33.15 (C_9), 19.82 and 19.11 (C_{10} and C_{11}), 11.64 (C_{12}); IR (film) 3198 cm^{-1} (amide NH), 2940 (CH), 1682 (amide C=O); EIMS (direct probe) m/e 179 (M^+), 164 ($\text{M}^+ - \text{CH}_3$), 136 ($\text{M}^+ - \text{HNCO}$), 108 ($\text{M}^+ - \text{HNCO} - \text{C}_2\text{H}_4$), 93 ($\text{M}^+ - \text{HNCO} - \text{C}_2\text{H}_4 - \text{CH}_3$).

7-Azabicyclo[4.2.1]nonan-8-one (4A) was prepared by reacting chlorosulfonyl isocyanate with cycloheptatriene in nitromethane according to the procedure of Malpass.^{18–20} The *N*-sulfonyl chloride so obtained was hydrolyzed using NaOH in aqueous acetone (pH 6–8), and was then hydrogenated with PtO_2/H_2 to yield the product, which was purified by silica gel column chromatography and HPLC on an ODS column with acetonitrile (4 mL/min) to yield a low-melting semicrystalline solid (57% yield): ^1H NMR (CDCl_3 , 300 MHz) δ 7.30 ppm (NH, bs, 1 H), 3.893 (H_6 , bdm [$J = 7.81$ Hz], 1 H), 2.480 (H_1 , ddd [$J = 8.30$, 6.35, 2.44 Hz], 1 H), 2.288 ($\text{H}_{9\text{epi}}$, bdt [$J = 12.21$, 8.30 Hz], 1 H), 1.95 (? , bm, 1 H), 1.838 ($\text{H}_{9\text{anti}}$, dd [$J = 12.70$, 0.98 Hz], 1 H), 1.7 and 1.58 (? , 2m, 3 H + 4 H); ^{13}C NMR (CDCl_3) δ 182.18 ppm (C_7), 53.20 (C_6), 40.22 (C_1), 35.37 (C_9), 30.87 and 30.22 (C_2 , C_5), 24.83 and 23.45 (C_3 , C_4); IR (film) 3250 cm^{-1} (amide NH), 2930 (CH), 1690 (C=O); EIMS (direct probe) m/e 139 (M^+), 111 ($\text{M}^+ - \text{CO}$), 96 ($\text{M}^+ - \text{HNCO}$).

General Method of Fluorination. Trifluoromethyl hypofluorite was contained in a 75-mL high-pressure (1880 psi) SS319 tank or the tank supplied by PCR Inc. and was equipped with a Hoke regulating SS319 valve attached to a Cajon SS319 tee, from which a stainless steel Matheson low/high pressure (–30 to +300 psi) gauge and a second Hoke valve was connected. The second valve was connected with Teflon tubing to a glass tee and on to a bubbler into a two-necked round-bottom flask (100 mL). The third side of the tee was connected to a dry nitrogen supply. The outlet of the flask was run into a basic solution of KI to trap and destroy any unreacted CF_3OF and the HF and COF_2 by-products of the reaction. The flask was further equipped with a magnetic stirrer and a cold bath.

The required amount of CF_3OF (determined from the change in the pressure of the calibrated volume²¹ between the two valves) was diluted with dry nitrogen before being slowly bubbled through the solution of the substrate contained in the flask. Chloroform and methylene chloride were used as solvents in the fluorinations here. The reactions were carried out in the presence of a small amount of anhydrous sodium carbonate at –70 to –20 $^{\circ}\text{C}$ (depending upon the solubility of the amide to be fluorinated) over a period of a few hours. Most of the unreacted starting amide could be removed by column chromatography on silica gel. Further purification of the material was achieved by HPLC using a semipreparative silica gel (Zorbax Sil) column with either methylene chloride or methanol as eluents.

Synthesis of 2-Fluoro-2-azabicyclo[2.2.2]octan-3-one (1B). 3-Isoquinolidone (0.008 mol, recrystallized from cyclohexane) was dissolved in chloroform (50 mL) and placed in the reaction vessel. After nitrogen was passed through the system for a few minutes, a pinch of anhydrous sodium carbonate was added and the solution cooled to dry ice/acetone temperature. CF_3OF (0.002 mol) diluted with nitrogen was bubbled through the solution slowly over a period of 3 h, the effluent gas exiting into basic KI solution. At the end of this time, the solution was allowed to equilibrate to room temperature as it was flushed with nitrogen. After the chloroform solution was treated with a saturated NaHCO_3 solution and washed with distilled water, the organic layer was separated and dried over anhydrous MgSO_4 . After filtration, the solvent was removed on a rotary evaporator without heat to yield a solid. Most of the unreacted amide was removed on a silica gel column, which was eluted successively with pentane, pentane–benzene (1:1), benzene–chloroform (4:1, then 2:1), and chloroform. The *N*-fluoroamide elutes during the benzene–chloroform mixtures and the unreacted amide elutes with chloroform. The spectroscopic sample was further purified by HPLC on a silica gel (Zorbax Sil) semipreparative column using CH_2Cl_2 as the eluent: ^1H NMR (CDCl_3 , 300 MHz) δ 4.146 ppm (H_1 , dtm [$J = 19.49$, 3.31 Hz], 1 H), 2.742 (H_4 , dtm [$J = 5.88$, 2.67 Hz], 1 H), 2.141 ($\text{H}_{6\text{endo}}$ and $\text{H}_{7\text{endo}}$, tdm [$J = 9.3$, 3.6 Hz], 2 H), 1.936 ($\text{H}_{6\text{exo}}$ and $\text{H}_{7\text{exo}}$, tdd [$J = 9.0$, 3.1, 1.4 Hz], 2 H), 1.86 (imp = impurity), 1.804 (m, 0.5 H), 1.75 (dm [$J = 9.5$ Hz], 3.5 H); ^{13}C NMR (CDCl_3) δ 60.9 ppm (C_1 , d [$^2J_{\text{CF}} = 2.9$ Hz]), 40.6 (C_4), 25.7 and 25.4 (C_6 and C_7 , $^3J_{\text{CF}} = 5.9$ Hz), 23.8 (C_5 and C_8); ^{19}F NMR (CDCl_3) δ 62.17 ppm (bd, $J = 19.5$ Hz);

(19) Malpass, J. R. *J. Chem. Soc., Chem. Commun.* 1972, 1246.

(20) Malpass, J. R.; Tweedle, N. J. *J. Chem. Soc., Perkin Trans. 1* 1976, 874.

(21) Calibration of the volume between the two valves was done by titration of the I_2 liberated from a known quantity of CF_3OF in KI solution with standard $\text{Na}_2\text{S}_2\text{O}_3$. As the volume was 7.14 ± 0.30 mL, the quantity of CF_3OF was $1.99 \pm 0.09 \times 10^{-5}$ mol/lb-in.²

(15) Pearlman, W. M. "Organic Syntheses", Collect Vol. V; Wiley: New York, 1973; pp 670–672.

(16) Malpass, J. R.; Tweedle, N. J. *J. Chem. Soc., Chem. Commun.* 1972, 1244.

(17) Graf, R.; Biener, H. *Angew. Chem., Int. Ed. Engl.* 1963, 2, 546.

(18) Malpass, J. R. *Tetrahedron Lett.* 1972(49), 4951.

IR (film) 2930 cm^{-1} (CH), 1740 (C=O), 1230 and 1170 (NF); EIMS (direct probe) m/e 143 (M^+), 125 ($\text{M}^+ - \text{F} + \text{H}$), 97 (125 - CO), 96 (97 - H), 82 (125 - NCO), 81 (82 - H), 69 (97 - C_2H_4), 68 (69 - H).

Synthesis of 4-Fluoro-4-aza-10,10-dimethyltricyclo[5.2.1.0^{1,5}]decan-3-one (2B). A N_2 -purged CHCl_3 (60 mL) solution of **2A** (0.003 mol) was placed in the reaction vessel and was cooled to -20°C with a dry ice/carbon tetrachloride bath. Then CF_3OF (0.001 mol) diluted with dry N_2 was bubbled slowly through the solution with continuous stirring. The reaction was allowed to equilibrate to room temperature with stirring overnight, after which time, the system was flushed with N_2 to remove the unreacted CF_3OF . Removal of the chloroform from the mixture resulted in a residue which was purified as described above: ^1H NMR (CDCl_3 , 300 MHz) δ 3.647 ppm (H_{5a} , ddd [$J = 21.74$ (21.40 decoupled from the ring hydrogens), 7.60, 4.23 Hz], 1 H), 2.293 (H_{2a} and H_{2b} , AA' d [$J_{\text{HF}} = 2.46$ Hz], 2 H), 2.297 (H_{6a} , m, 1 H), ca. 1.92 (H_7 , H_{8a} , and H_{9a} , m, 3 H), 1.70 (H_{6a} , dd [$J = 13.4$, 7.65 Hz], 1 H), 1.37 (H_{9a} , dt [$J = 12.5$, 9.0 Hz], 1 H), ca. 1.32 (H_{8a} , m, 1 H), 1.08 and 0.95 (H_{11} and H_{12} , 2s, 6 H); ^{13}C (CDCl_3) δ 69.58 ppm (C_5 , $^2J_{\text{CF}} < 1$ Hz), 56.9 (C_1), 46.96 (C_{10}), 35.9 (C_7), 33.70 (C_9), 30.48 (C_2 , d, $^3J_{\text{CF}} = 4.4$ Hz), 28.18 (C_8), 22.00 and 20.70 (C_{11} and C_{12}); ^{19}F NMR (CDCl_3) δ 72.0 ppm (d, $^3J_{\text{NF-CH}} = 23.4$ Hz); IR (film) 2970 cm^{-1} (CH), 1745 (C=O), 1015, 1000, and 860 (NF); EIMS (direct probe) m/e 179 ($\text{M}^+ - \text{F} + \text{H}$), 164 (179 - CH_3), 151 (179 - CO), 136 (164 - C_2H_4), 124 (151 - $\text{C}_2\text{H}_2 - \text{H}$), 109 (124 - CH_3), 96 (124 - C_2H_4), 93 (151 - $2\text{C}_2\text{H}_4$).

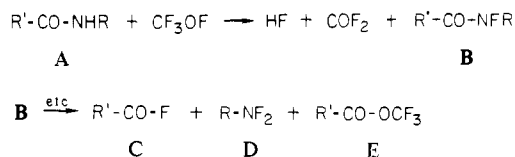
2-Fluoro-2-aza-7,7,8-trimethyltricyclo[4.2.1.0^{4,8}]nonan-3-one (3B) was prepared by treating CF_3OF (0.001 mol) with **3A** (0.003 mol) in CHCl_3 at dry ice/acetone temperature. The compound was purified as described above: ^1H NMR (CDCl_3 , 300 MHz) δ 3.892 ppm (H_1 , dd [$J = 7.45$, 1.01 Hz], 1 H), 2.377 ($\text{H}_{5\beta}$, d_{AB}td [$J = 11.03$, 3.31, 2.02 Hz], 1 H), 2.313 (H_4 , d_{AB}m [$J = 11.12$ Hz], 1 H), ca. 2.0 ($\text{H}_{9\beta}$, mm, 1 H), 1.941 (H_6 , dd [$J = 3.03$, 1.38 Hz], 1 H), 1.607 (H_{5a} , d [$J = 11.77$ Hz], 1 H), 1.582 (H_{9a} , dd [$J = 13.6$, 1.47 Hz], 1 H), 1.175 (H_{10} , s, 3 H), 0.984 and 0.948 (H_{11} and H_{12} , 2s, 6 H); ^{13}C NMR (CDCl_3) δ 177.55 ppm (C_3 , d, $^2J_{\text{CF}} = 9.6$ Hz), 66.26 (C_1 , d, $^3J_{\text{CF}} = 2.9$ Hz), 51.12 (C_8 , d, $^3J_{\text{CF}} = 4.4$ Hz), 48.36 (C_7), 46.21 (C_6), 45.48 (C_4 , d, $^3J_{\text{CF}} = 5.1$ Hz), 35.81 (C_5), 31.57 (C_9 , d, $^3J_{\text{CF}} = 3.7$ Hz), 19.19 (C_{10} , d, $^3J_{\text{CF}} = 2.2$ Hz), 18.95 (C_{12}), 11.96 (C_{11}); ^{19}F NMR (CDCl_3) δ 73.16 ppm (bs); IR (film) 2980 cm^{-1} (CH), 1750 (C=O), 998 and 850 (N-F); EIMS (direct probe) m/e 197 (M^+), 179 ($\text{M}^+ - \text{F} + \text{H}$), 169 ($\text{M}^+ - \text{CO}$), 164 (179 - CH_3), 150 ($\text{M}^+ - \text{CO} - \text{F}$).

7-Fluoro-7-azabicyclo[4.2.1]nonan-8-one (4B) was prepared by the reaction of CF_3OF (0.0010 mol) with **4A** (0.0036 mol) in CHCl_3 at dry ice/acetone temperature as previously described. The product was purified as described above: ^1H NMR (CDCl_3 , 300 MHz) δ 4.228 ppm (H_6 , dt [$J = 6.85$, 2.95 Hz], 1 H), 2.564 (H_1 , bt [$J = 8.0$ Hz], 1 H), ca. 2.28 ($\text{H}_{9\text{epi}}$ and $\text{H}_{5\beta}$, m, 2 H), ca. 2.08 ($\text{H}_{4\beta}$, dddd [$J = 12.9$, 7.6, 3.0, 1.1 Hz], 1 H), 1.895 ($\text{H}_{9\text{anti}}$, d [$J = 12.7$ Hz], 1 H), 1.895 ($\text{H}_{9\text{anti}}$, d [$J = 12.7$ Hz], ca. 1 H), 1.86-1.63 ($\text{H}_{2\beta}$, $\text{H}_{3\beta}$, and H_{2a} , mm, ca. 3 H), 1.6-1.4 (H_{3a} and H_{5a} , mm, 2 H), ca. 1.29 (H_{4a} , qd [$J = 12.2$, 2.4 Hz], 1 H) and impurities at 1.92 (d, $J = 13.2$ Hz), 1.258 (H_2O) and 0.89 (m, 0.3 H); ^{13}C NMR (CDCl_3) δ 58.92 ppm (C_6 , d, $^2J_{\text{CF}} = 4.4$ Hz), 35.41 (C_1 , d, $^3J_{\text{CF}} = 3.7$ Hz), 30.78 (C_9 , d, $^3J_{\text{CF}} = 7.4$ Hz), 30.26 ($\text{C}_{2\beta}$), 24.60 ($\text{C}_{3\beta}$), 24.21 (C_5 , d, $^3J_{\text{CF}} = 5.9$ Hz), 22.16 ($\text{C}_{4\beta}$); ^{19}F NMR (CDCl_3) δ 81.70 ppm (bs); IR (film) 2930 cm^{-1} (CH), 1746 (C=O), 980 and 906 (N-F); EIMS (direct probe) m/e 157 (M^+), 139 ($\text{M}^+ - \text{F} + \text{H}$), 138 ($\text{M}^+ - \text{F}$), 114 ($\text{M}^+ - \text{NCO}$), 110 (138 - CO), 97 (139 - NCO).

N-Fluoro- ϵ -caprolactam (5B) was originally synthesized by Grakauskas et al.²² by the direct fluorination. It was prepared here by reaction of CF_3OF (0.0022 mol) with ϵ -caprolactam (0.0044 mol) in CH_2Cl_2 at dry ice/2-propanol temperature. The product oil was purified by the procedure described above: ^1H NMR (CDCl_3) δ 3.92 ppm (H_6 , dm [ring H's decoupled $J = 28.17$ Hz], 2 H), 3.52 (H_2 , bm [$\text{H}_{3,5}$ decoupled $J = 2.64$ Hz], 2 H), 2.84 (H_5 , bm, 2 H), 2.76 (H_3 and H_4 , bm, 4 H); ^{13}C NMR (CDCl_3) δ 174.28 ppm (C_1 , d, $^2J_{\text{CF}} = 4.5$ Hz), 54.73 (C_6 , d, $^2J_{\text{CF}} = 11.0$ Hz), 35.35 (C_5 , d, $^3J_{\text{CF}} = 1.7$ Hz), 29.37 (C_4 or C_3), 26.53 (C_2 , d, $^3J_{\text{CF}} = 3.3$ Hz), 23.28 (C_3 or C_4); ^{19}F NMR (CDCl_3) δ 42.44 ppm (t, $J = 28.7$ Hz); IR (film) 2940 cm^{-1} (CH), 1705 (C=O), 1070, 988, 938, and 850 (N-F); EIMS (direct probe) m/e 131 (M^+), 113 ($\text{M}^+ - \text{F} + \text{H}$), 85 (113 - CO), 84 (85 - H).

N-Fluoro-2-pyrrolidone (6B) was also synthesized by Grakauskas et al.²² by direct fluorination of 2-pyrrolidone (**6A**). It was prepared by the reaction of CF_3OF (0.004 mol) with **6A** (0.012 mol) in CH_2Cl_2 at dry ice/acetone temperature and purified by the procedure described earlier: ^1H NMR (CDCl_3 , 300 MHz) δ 3.709 ppm (H_5 , dt [$J = 8.58$, 6.76 Hz], 2 H), 2.383 (H_3 , tdm [$J = 7.95$, 3.00 Hz], 2 H), 2.14 (H_4 , pm [$J = 6.8$ Hz], 2 H), H_4 decoupled yields two doublets ($J = 8.58$ and 3.00 Hz) for H_5 and H_3 , respectively; ^{19}F NMR (CDCl_3) δ 69.81 ppm (bm); IR (film) 1745 cm^{-1} (C=O).

Scheme I



N-Fluoro-2-piperidone (7B) was also isolated by Grakauskas et al.²² from the direct fluorination of 2-piperidone (**7A**). It was prepared by the reaction of CF_3OF (0.0034 mol) with **7A** (0.010 mol) in CHCl_3 at dry ice/acetone temperature and then purified by the procedure outlined above: ^1H NMR (CDCl_3) δ 3.75 ppm (H_6 , dt [$J = 9.2$, 5.9 Hz], 2 H), ca. 2.46 (H_3 , td [$J = 5.9$, 4.7 Hz], 2 H), ca. 1.7 (H_4 and H_5 , bm, 4 H); ^{19}F NMR (CDCl_3) δ 50.62 ppm (bs).

N-Fluoro-N-tert-butylformamide (8B) was prepared by reaction of CF_3OF (0.010 mol) with *N-tert*-butylformamide (0.040 mol) in CHCl_3 in the presence of a pinch of anhydrous Na_2CO_3 at dry ice/acetone temperature and was purified by the procedure described above. The product oil is very sensitive to acid: ^1H NMR (CDCl_3) δ 8.436 ppm ($\text{H}_{\text{C=O}}$, d [$J = 18.47$ Hz], 1 H), 1.472 ($\text{H}_{\text{t-Bu}}$, d [$J = 1.32$ Hz], 9 H); ^{13}C NMR (CDCl_3) δ 160.1 ppm (C=O, bs, $^2J_{\text{CF}} = \text{ca. } 0$ Hz), 30.7 (C_1 , d, $^2J_{\text{CF}} = 14.7$ Hz), 28.5 (3C, d, $^3J_{\text{CF}} = 4.4$ Hz); ^{19}F NMR (CDCl_3) δ 67.74 ppm (d, $J = 16.9$ Hz).

N-Fluoro-N-methylstearamide (9B) was prepared by the method of Barton et al.¹ via the reaction of CF_3OF (0.003 mol) with *N*-methylstearamide (0.0018 mol) in CHCl_3 at room temperature: ^1H NMR (CDCl_3) δ 3.35 ppm (H_{NMe} , d [$J = 27.11$ Hz], 3 H), 2.43 (H_2 , td [$J = 6.4$, 5.13 Hz], 2 H), 1.39 ($[\text{CH}_2]_{16}$, bs, 32 H), 0.86 (H_{18} , bt [$J = \text{ca. } 7$ Hz], 3 H); ^{19}F NMR (CDCl_3) δ 55.8 ppm (qbt, $J = 28.5$, ca. 5 Hz).

Ethyl *N*-fluoro-*N*-acetylglucinate (**10B**) was prepared from ethyl *N*-acetylglucinate by Reid²³ using the procedures described above. ^{19}F NMR (CDCl_3) δ 55.5 ppm (tq, $J = 31.90$, 7.03 Hz).

Results and Discussion

Synthesis of N-Fluoroamides. Barton et al.¹ synthesized various *N*-fluoro compounds using trifluoromethyl hypofluorite (CF_3OF) and difluoromethylene dihypofluorite [$\text{CF}_2(\text{OF})_2$] as the fluorination reagents. The conditions under which they treated trifluoromethyl hypofluorite with amides gave *N*-fluoroamides (**B** in Scheme I) only in low yields. Other products such as the *N,N*-difluoroamine (**D**), the acid fluoride (**C**), and the trifluoromethyl ester (**E**) were also isolated from the reaction (see Scheme I). By varying the reagent concentrations, they showed that products **C**, **D**, and **E** were formed by further reaction of **B** with the reagent. Apparently the monofluoroamide reacts with the reagent competitively with, or faster than, **A**. These authors also suggested that the mechanism of the fluorination probably involved an initial attack of the N lone-pair electrons of **A** or **B** on the O-F bond of the reagent to give F^- , COF_2 , and an N tetrahedral intermediate which loses H^+ to the F^- yielding **B**. Our observations here are completely consistent with this mechanism.

In order to maximize the yield of the monofluoroamide and minimize the yield of the secondary products, we have optimized the conditions as shown below (a-c).

(a) The reaction was performed in chloroform or methylene chloride solutions, constantly purged with dry N_2 gas, and cooled to dry ice/acetone (-76°C) or dry ice/carbon tetrachloride (-20°C) depending upon the solubility of the amide to be fluorinated.

(b) At least a 3:1 excess of amide: CF_3OF was used instead of the 1:1 ratio used by the previous authors,¹ and the CF_3OF was diluted with the purge N_2 at least 1:10 times.

(c) In certain cases, especially with formamides, a few milligrams of anhydrous sodium carbonate was added to the reaction. The function of the added solid is not clear, but it probably removes traces of moisture and some by-product HF, and helps prevent hydrolysis.

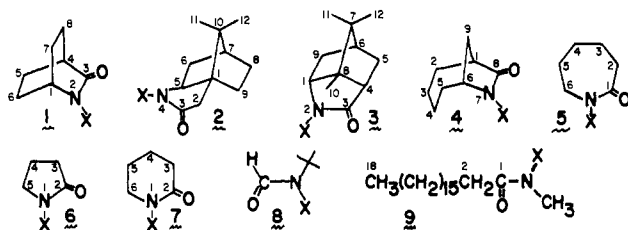
The above modifications provide 50-70% yields (based on CF_3OF) of the *N*-fluoroamides, and the often expensive starting

Table I. Spectral Data of the Model Amides^a

compd no. ^b	position α to N				position α to C=O				N-F δ_F	C=O			
	$\delta_H, X =$		$\delta_C, X =$		$\delta_H, X =$		$\delta_C, X =$			$\delta_C, X =$		IR, ν (cm ⁻¹)	
	H	F	H	F	H	F	H	F		H	F	H	F
1	3.63	4.146 (19.49)	47.64	60.9 (2.9)	2.48	2.742 (5.88)	37.89	40.6 (ca. 0)	62.17 (19.5)	178.77		1680	1740
2	3.492	3.647 (21.74)	64.61	69.58 (<1)	2.243, 2.103	2.293 (2.46)	28.40	30.48 (4.4)	72.0 (23.4)	180.37		1700	1745
3	3.37	3.892 (ca. 0.6)	60.64	66.56 (2.9)	2.18	2.313 (1.1)	47.51	45.77 (5.1)	73.16	183.29	178.84 (9.6)	1682	1750
4	3.893	4.228 (ca. 0.2)	53.20	58.92 (4.4)	2.480	2.564 (ca. 0)	40.22	35.51 (3.7)	81.70	182.18		1690	1746
5	3.17	3.92 (28.18)		54.73 (11.0)	2.38	3.52 (2.64)		26.53 (3.3)	42.44 (28.7)		174.28 (4.5)	1660	1705
6		3.709 (8.58)	40.1			2.383 (3.00)	28.9		69.81	179.2		1700	1745
7	3.23	3.75 (9.34)	42.2		2.28	2.46 (4.7)	31.4		50.62	174.3			
8			51.1	30.7 (14.7)	8.27 ^c	8.43 ^d (18.47)			67.74	164.1	160.1		
9	2.81	3.35 (27.11)			2.14	2.43 (5.13)			55.8 (28.5, ca. 5)				

^a Chemical shifts of ¹H and ¹³C data are ppm downfield from internal Me₄Si; ¹⁹F chemical shifts are ppm downfield from external CFCl₃ and all fluorine coupling constants are in parentheses (Hz). ^b Compound numbers as in text where X = H is A and X = F is B. ^c The *cis*-formyl hydrogen is reported, although a 53:47 *cis*:*trans* peptide bond mixture was observed ($J_{cis} = 12.3$, $J_{trans} = 2.0$ Hz). ^d The formyl hydrogen is reported (>99% *cis* peptide was obtained); a long $^4J_{HF} = 1.32$ Hz to the *tert*-butyl methyls was also observed.

materials could be recovered almost quantitatively to be recycled. When near-equimolar quantities were used, mostly intractable mixtures were obtained, strongly suggesting that the mono-fluoroamide fluorinates (or decomposes under the reaction conditions) faster than the starting amide. Once isolated, the *N*-fluoroamides are quite stable and can be stored indefinitely at -20 °C except the *N*-fluoroformamides, which slowly decompose even at this temperature. The fluoroamides (1-9) used in this study



X = H, series A; X = F, series B

were prepared from known amides.^{1,15-20,23} This series of compounds was chosen because the amides are nearly rigid and provide several unique $<90^\circ$ bond angles, but unfortunately no $>90^\circ$ angles are present except for compound **5**, which is an average of at least two conformations. It is hoped that cyclic peptides will provide the $>90^\circ$ models later.

NMR Studies. As can be seen in Table I, a combination of ¹H and ¹³C NMR spectral data was particularly useful in identifying a fluorine atom attached to the molecule. The changes in chemical shifts and the additional coupling in both the ¹H and ¹³C spectra are clear indicators of replacing the N-H with N-F. In general, the following changes occur in the spectral data for the *N*-fluoroamide vs. the amide.

1. The amide broad proton signal disappears.
2. The C-H adjacent to the NF moves downfield 0.48 ± 0.19 ppm (range 0.16-0.77 ppm). This is attributed to the inductive withdrawal of electron density caused by the F atom and is confirmed by the downfield shift of the ¹³C resonance of 7.21 ± 4.25 ppm (range 4.4-20.4 ppm) although the latter could also be due to a paramagnetic contribution from the ¹⁹F atom.
3. The effect is also transmitted across the C=O group to the other C₂H, which moves downfield 0.31 ± 0.37 ppm (range 0.12-1.14 ppm), but our inability to assign some of the carbons with confidence prevents any generalization of the ¹³C data at this time.

4. The carbonyl carbon moves upfield ca. 4 ppm, and the IR stretching frequency increases by 53 ± 9 cm⁻¹. The latter is probably due to an inductive effect through the σ bonds, but the former is thought to be evidence for back-donation of the p orbitals of the F atom into the π -electron system of the peptide bond and may account for some of the unusual fluorination chemistry observed.

5. ¹⁹F-¹H couplings are observed; the three-bond couplings were 0-31.90 Hz and the four-bond couplings were 0-7.03 Hz, but both ranges are much smaller than should be expected. Based on our free rotation couplings of 27.11 to 31.9 and 5.1 to 7.0 Hz and our determined 60° angle values from **6B** of 8.58 and 3.00 Hz for the three-bond and four-bond couplings, respectively, one can predict the magnitude of J_{180° from

$$J_{180^\circ} = 3J_{free} - 2J_{60^\circ} \quad (2)$$

to be ± 64.1 and ± 78.5 (if the signs of J_{free} and J_{60° are the same) or ± 98.5 and ± 112.9 Hz (if signs are opposite) for the three-bond coupling of the ϕ' angle, and ± 9.6 or ± 15.0 (same signs) or ± 21.3 or ± 27.0 Hz (opposite signs) for the four-bond coupling of the ψ' angle. For reasons that will be developed below, we believe that the opposite sign cases are correct for both the ϕ' and ψ' angles.

6. Several two-bond and three-bond ¹⁹F-¹³C couplings are also observed: $^2J_{FN-C_\alpha} = <1.0$ to 14.7 Hz, $^2J_{FN-C=O} = 4$ to 9.6 Hz, $^3J_{FN-CO-C_\alpha} = 0$ to 5.1 Hz, and $^3J_{FN-C_\alpha-C_\beta} = 2.2$ to 7.4 Hz. As more data are obtained it should be possible to develop new Karplus relations for the three-bond couplings, but at the moment the couplings assist greatly in assigning the ¹³C resonances.

7. Finally, the ¹⁹F resonances of our model compounds vary over a large chemical shift range (42.44-81.70 ppm downfield of external CFCl₃), but only couplings of >5 Hz are observable because of the quadrupolar broadening caused by the ¹⁴N atom. The ¹⁹F spectra of **2B**, **5B**, and **9B** are shown in Figure 1. Note that only the quartet ($^3J = 27.11$ Hz) of **9B** shows any hint of extra coupling ($^4J = 5.13$ Hz), whereas neither the triplet ($^3J = 28.17$ Hz) of **5B** nor the doublet ($^3J = 21.74$ Hz) of **2B** shows any hint of the smaller 2.64 and 2.46 Hz four-bond couplings, respectively, that were obtained from the ¹H spectra.

Choice of Models. The compounds used as models for the determination of the Karplus relationships reported here were chosen partly for their rigidity, expected ϕ' and ψ' angles, and ease of preparation of known structures. For the purposes of this determination, the fluorinated amide system was assumed to be

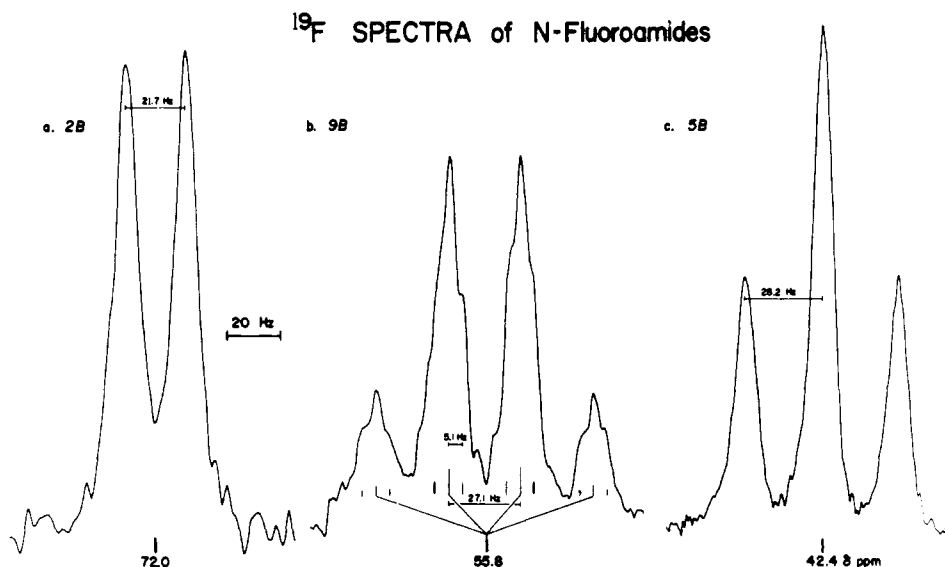
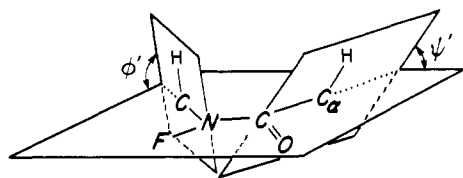


Figure 1. ^{19}F NMR spectra of selected *N*-fluoroamides at 84.70 MHz in CDCl_3 downfield from external CFCl_3 : (a) 4-fluoro-4-aza-10,10-dimethyltricyclo[5.2.1.0^{1,5}]decan-3-one (**2B**), (b) *N*-fluoro-*N*-methylstearamide (**9B**), and (c) *N*-fluoro- ϵ -caprolactam (**5B**).

planar. The definition of the ϕ' and ψ' angles as used here is given in the diagram below. The ϕ' and ψ' angles were determined



as the intersections of the $\text{N}-\text{C}-\text{H}$ plane and the $\text{C}(\text{O})-\text{C}_\alpha-\text{H}$ plane with the *N*-fluoroamide bond plane, respectively. It is, of course, recognized that peptide bonds may not be strictly planar from the work of Ramachandran et al.,²⁴ who have shown that the $\text{N}-\text{H}$ bond can be $\pm 15\text{--}20^\circ$ out of the plane of the carbonyl. These angular deviations are probably the reasons for the scattering in the Karplus curves that are derived below. As more data become available, these curves will undoubtedly be improved.

The ϕ' and ψ' angles were obtained by empirically measuring carefully straightened Dreiding models of the compounds synthesized. These angles and the corresponding experimental $^1\text{H}-^{19}\text{F}$ couplings are presented in Table II. The angles for **5B** were obtained from the published X-ray data²⁵ of the $\text{N}-\text{H}$ analogue **5A**, as the fluorine atom is only 40% larger than a hydrogen atom.

Our 0° model **1B** for both ϕ' and ψ' has been used previously by several groups^{4,26} for the ϕ' $\text{NH}-\text{C}_\alpha\text{H}$ Karplus relationship. We have constrained our derived Karplus curve fitting to force the curves to start at $^3J_{0^\circ} = 19.5$ Hz and $^4J_{0^\circ} = (-)5.9$ Hz to reflect our confidence in this angle by applying the restriction of eq 3 to eq 1:

$$A + B + C = J_{0^\circ} \quad (3)$$

Model **3B** was initially synthesized to obtain a $30\text{--}45^\circ$ model, but the observed couplings were near zero, which surprised us. Therefore, **4B** was synthesized to confirm that the $30\text{--}40^\circ$ angle couplings were very small (see Table II). The magnitude of these couplings were estimated from line narrowing that occurred during a CW fluorine heteronuclear decoupling experiment. In the next section, a few of these experiments will be illustrated on our new

Table II. Derived ϕ' and ψ' Angles and Coupling Constants of the Model *N*-F-fluoroamides

compd no.	ϕ' angle (deg)		ψ' angle (deg)	
	molecular models ^b	$^3J_{\text{HF}}$ (Hz)	molecular models ^b	$^4J_{\text{HF}}$ (Hz)
1B	0.0	19.5	0.0	5.9
2B	80.0	21.7	45.0, 75.0	2.5 ^c
3B	35.0	0.6 ^d	35.0	1.1
4B	37.5	0.2 ^d	37.5	0.0
5B	2.2, 116.3 ^f	28.2 ^e	2.6, 116.1 ^f	2.6 ^e
6B	60.0, 60.0	8.6	60.0, 60.0	3.0
7B	45.0, 75.0, 80.0, 40.0	9.3 ^e	80.0, 40.0, 45.0, 75.0	4.7 ^e
9B	free	27.1 ^e	free?	5.1 ^e
10B ^g	free	31.9 ^{e,g}	free	7.0 ^{e,g}

^a Compound numbers as in text and Table I. ^b Estimated from carefully straightened Dreiding models and assumed a planar peptide bond (see text). ^c These two protons have identical chemical shifts, i.e., are an $\text{AA}'\text{F}$ system. ^d Estimated from the peak narrowing caused by decoupling the F atom. ^e When more than one conformation was expected to be in equilibrium, the observed J was considered as an average of an equal population of the reasonable conformations. ^f From the $\text{N}-\text{H}$ analogue X-ray data of Winkler and Dunitz.²⁵ ^g Data for compound **10B** (ethyl *N*-fluoro-*N*-acetylglucinate) was kindly provided by Miss Alice L. Reid.²³

80° model compound, **2B**, which was chosen to give us a near- 90° model that has been lacking in most previous ϕ' angle Karplus relations.

Analysis of the NMR Spectra. Assignments of the NMR resonances and ultimate extraction of the desired couplings were fairly routine although frequently time consuming, depending on the complexity of the structures. Unfortunately 2D-FT facilities were not available to us when this work was done, so many homonuclear decoupling experiments were required for the unequivocal assignment of the proton resonances. In addition, some of the ^{13}C resonances are not as certain, but the $\text{C}-\text{F}$ couplings greatly assisted the assignments of the *N*-fluoroamides. Generally ^1H , ^{13}C , and, when appropriate, ^{19}F NMR spectra were obtained on each compound.

For illustrative purposes, we will consider the ^1H spectra of the **2A**, **2B** pair of amides. The 300-MHz ^1H spectrum of **2A** is shown in Figure 2. The ϕ' angle proton (5α) located at δ 3.492 ppm does not have a measurable coupling to the NH , but it is coupled to 6α ($^3J = 8.2$ Hz) and to 6β ($^3J = 4.7$ Hz), which are located at 1.63 and 1.95 ppm, respectively. The two-bond geminal coupling of the 6α and 6β hydrogens is 12.9 Hz. Note that $\text{H}_{6\beta}$ has

(24) (a) Ramachandran, G. N.; Lakshminarayanan, A. V.; Kilaskai, A. S. *Biochim. Biophys. Acta* 1973, 303, 8-13. (b) Ramachandran, G. N.; Kolaskar, A. S. *Ibid.* 1973, 303, 385-8.

(25) Winkler, F. K.; Dunitz, J. D. *Acta Crystallogr., Sect. B* 1975, 31, 268.

(26) (a) Ramachandran, G. N.; Chandrasegaran, R.; Kopple, K. D. *Biopolymers* 1971, 10, 2113. (b) Cung, M. T.; Marraud, M.; Neel, J. *Macromolecules* 1974, 7, 606.

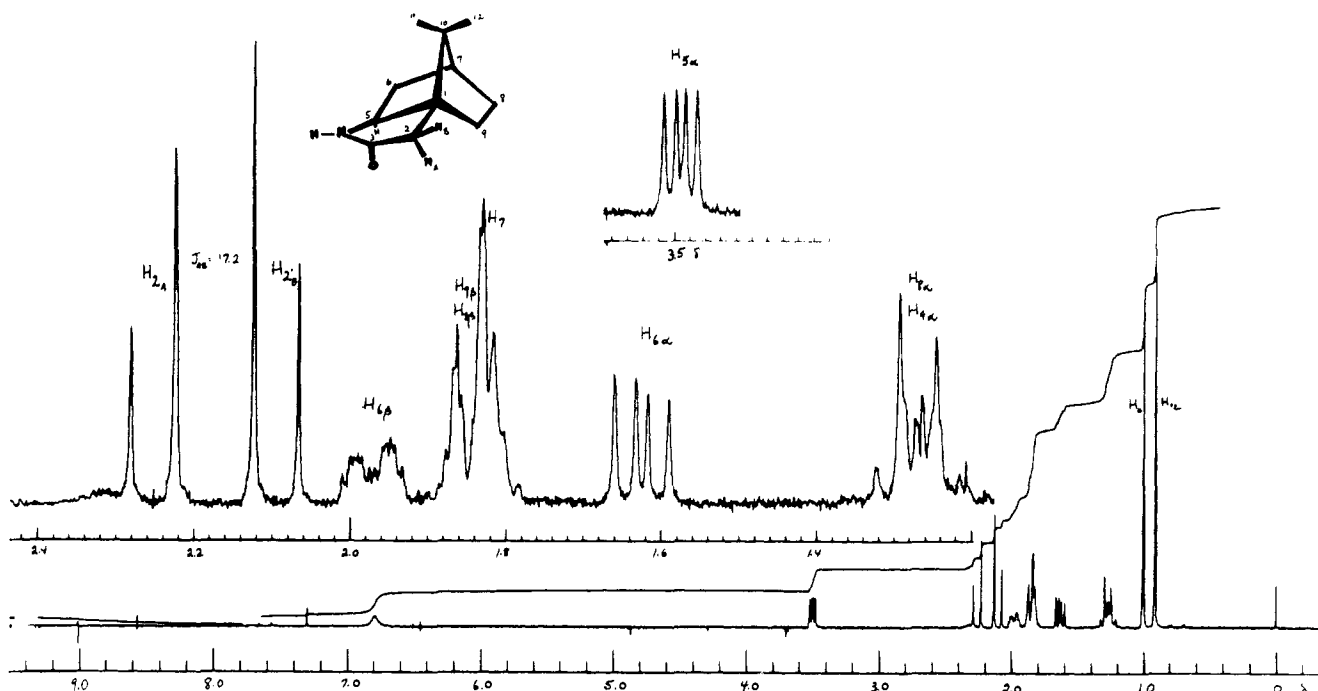


Figure 2. ^1H NMR spectrum of 4-aza-10,10-dimethyltricyclo[5.2.1.0^{1,5}]decan-3-one (**2A**) at 300 MHz in CDCl_3 downfield from internal $\text{Si}(\text{CH}_3)_4$.

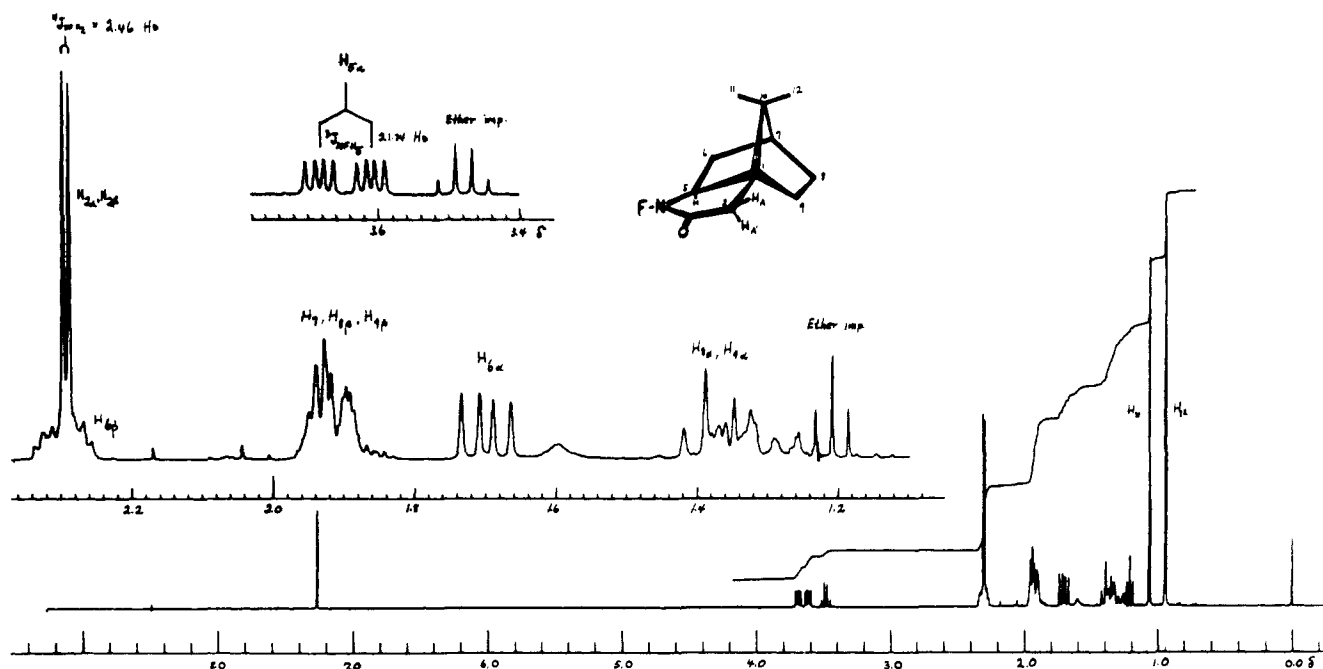


Figure 3. ^1H NMR spectrum of 4-fluoro-4-aza-10,10-dimethyltricyclo[5.2.1.0^{1,5}]decan-3-one (**2B**) at 300 MHz in CDCl_3 downfield from internal $\text{Si}(\text{CH}_3)_4$.

further small couplings to H_7 at 1.82 ppm and $\text{H}_{8\beta}$ at 1.84 ppm. The two ψ' angle protons (2α and 2β) are located at 2.243 and 2.103 ppm ($^2J_{\text{AB}} = 17.24$ Hz) with the low-field resonance slightly broadened, presumably from long-range coupling from the NH. The actual assignment of these two protons would be important if different ^1H - ^{19}F couplings were observed in the spectrum of **2B**. The possibility of obtaining two ψ' angles in one compound was one of the reasons this model was chosen because it should have been possible to determine the signs of the H-F coupling constants from the appropriate spin-tickling experiments. Unfortunately, these two protons in **2B** have coincidental chemical shifts and therefore become an AA'X system (where X = ^{19}F) at 2.293 ppm as shown in Figure 3. Since the peaks at 2.29 ppm integrated to three protons, another proton ($\text{H}_{6\beta}$) is under the doublet. To prove that this doublet ($^4J_{\text{HF}} = 2.46$ Hz) was due to the ψ' angle coupling from the N-F and not a highly distorted

AB quartet with the small outer peaks buried in the $\text{H}_{6\beta}$ resonance, the ^{19}F atom was decoupled at 84 699 746.0 Hz as shown in Figure 4c (WH-90 using a CDCl_3 lock with f_1 at 90.02325 MHz and the proton-decoupling coils returned to 84.7 MHz). Upon ^{19}F irradiation, the doublet at 2.293 ppm collapsed to a singlet, and the original eight-line pattern for $\text{H}_{5\alpha}$ at 3.647 ppm collapsed to the same four-line pattern observed $\text{H}_{5\alpha}$ of **2A** (Figure 2), thus proving the extra coupling came from the F atom and the two ψ' angle protons on C_2 were accidentally equivalent as suspected. This means that the observed $^4J_{\text{HF}}$ coupling is an average of J_{AF} and $J_{\text{A'F}}$.

The large coupling ($^3J_{\text{HF}} = 21.4$ Hz at 90 MHz and 21.74 Hz at 300 MHz) in the eight-line pattern of $\text{H}_{5\alpha}$ in the spectrum of **2B** (Figure 3 or 4a) was also determined by decoupling all of the ring protons with a high-power home-built homonuclear decoupler²⁷ as shown in Figure 4b. In this example, the ψ' angle protons

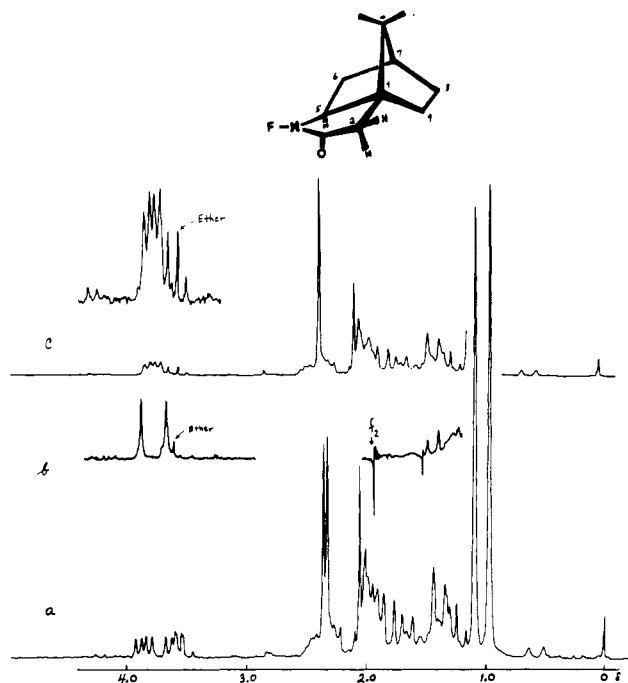


Figure 4. ^1H NMR spectra of 4-fluoro-4-aza-10,10-dimethyltricyclo-[5.2.1.0]^{1,5}decan-3-one (**2B**) at 90 MHz in CDCl_3 downfield from internal $\text{Si}(\text{CH}_3)_4$: (a) normal spectrum, (b) high-power homonuclear decoupling of all ring protons, and (c) ^{19}F heteronuclear decoupling at 84 699 746.0 Hz.

(H_2) were also irradiated to decouple the superimposed $\text{H}_{6\beta}$, but in most of the other model compounds it was possible to obtain the ψ' couplings by a similar broad-band CW ^1H decoupling experiment. The ϕ' and ψ' angle proton data are given in Table I and the complete spectra are reported in the Experimental Section.

The ^{19}F NMR spectra were routine, but only couplings larger than 5 Hz were observable because of the quadrupolar broadening due to the ^{14}N atom in the amide. The chemical shifts, which are also given in Table I, vary from δ 81.70 to 42.44 ppm downfield of external CFCl_3 . An attempt to selectively irradiate specific ^{19}F transitions was unsuccessful, as was an attempt to decouple the ^{14}N atom. The latter met with an unexpected difficulty: the high-power modulated ^{14}N frequency at 6.5 MHz contained a sufficient first overtone component to overload the deuterium lock at 13.8 MHz. While this latter problem was overcome with a crystal filter, the experiment was still unsuccessful, but further work is in progress.

Our ^{13}C NMR studies suggest that ^{13}C spectra will be very useful in identifying the location of a fluorine atom in a polypeptide because of the ^{13}C - ^{19}F couplings and the changes in chemical shifts on fluorination of the amide. Figure 5 gives the proton-decoupled ^{13}C spectrum of **3B**, which will be compared with the spectrum of **3A**. The carbonyl C of **3B** is a doublet ($^2J_{\text{CF}} = 9.6 \pm 0.7$ Hz) at 177.55 ppm compared to 183.29 ppm for the C=O of **3A**. The carbon adjacent to the nitrogen (C_1) is a doublet ($^2J_{\text{CF}} = 2.9$ Hz) at 66.26 ppm compared to 60.64 ppm for C_1 of **3A**. The carbon (C_4) adjacent to the C=O is a doublet ($^3J_{\text{CF}} = 5.1$ Hz) at 45.48 ppm compared to 47.51 ppm for C_4 of **3A**. Other three-bond C-F couplings have been observed for C_8 ($J = 4.4$ Hz) at 51.12 ppm and C_9 ($J = 3.7$ Hz) at 31.57 ppm. One four-bond C-F coupling to C_{10} ($J = 2.2$ Hz) at 19.19 ppm was also observed. These couplings greatly assist the assignment of the resonances, but when there were fewer C-F couplings the assignment was not as certain.

(27) The high-power homodecoupler was built by William H. Craig of our departmental electronics shop and is based on the usual timeshare principle but with a variable decoupling window so that one can experimentally determine a noninterference amount of power that will accomplish the desired decoupling experiment.

When 2D-FT becomes available to us, this problem will be considerably less difficult. The other ^{13}C spectral data were analyzed in a similar manner and are reported in part in Table I and completely in the Experimental Section.

In contrast to the rigid compounds discussed above, it is pertinent to consider a conformationally mobile compound, *N*-fluoro- ϵ -caprolactam (**5B**). Decoupling of all protons except H_6 ($\text{NF}-\text{C}_\alpha\text{H}$) resulted in a sharp doublet ($^3J_{\text{HF}} = 28.15$ Hz) for this H_6 resonance. If **5B** was one particular conformation, the protons of H_6 would be nonequivalent and should result in the AB part of an ABX pattern. Since only a simple doublet was observed, **5B** must be conformationally mobile wherein the interconversion of these protons are rapid with an almost equal population of both forms. An X-ray structure of **5A** (a chair conformation) has been reported,²⁵ in which the ϕ' angles are 2.2 and 116.3°, and the ψ' angles are 2.6 and 116.1°. In another experiment, all the protons except H_2 and H_6 were decoupled. Now the H_2 protons appeared as a simple doublet ($^4J_{\text{CF}} = 2.64$ Hz) for the ψ' angle coupling. The angles determined from the X-ray structure were used in the Karplus equation derivations.

One other long-range coupling constant was observed in the ^1H spectrum of **8B** between the N-F and the *tert*-butyl protons ($^4J_{\text{HF}} = 1.32$ Hz). This corresponds to a combination $\phi\chi_1$ peptide angle that might be useful in identifying which solution (low or high angle) of ϕ' in eq 1 is correct at some future time.

Nonlinear Least-Squares Fit of the ϕ' and ψ' Karplus Relations. Table II gives the estimated angular data based on Dreiding molecular models and the determined ^1H - ^{19}F coupling constants for the ϕ' and ψ' angles. The molecular model angles are probably within $\pm 5^\circ$. Since at least four angles were expected for the various twist-chair conformations of **7B**, it was not included in the Karplus equation fits. On the other hand, the rigid tricyclic models **2B** and **3B** were included since only one conformation for each was expected. Both **1B** and **4B** were expected to have rapidly equilibrating average angles of relatively small conformational changes ($< \pm 6^\circ$)^{26a} due to molecular twisting and were therefore used in the least-squares fits. Ramachandran^{26a} has argued that the solution equilibrium values of **1A** would be 0° for both the ϕ' and ψ' angles even though the X-ray structure values are 5.5 and 0.06° , respectively.

If the Fermi contact term is the dominating contribution to the ^1H - ^{19}F coupling constant, then the sign of $^3J_{\text{HF}}$ is expected to be positive and the sign of $^4J_{\text{HF}}$ should be negative. Using the above assumptions, we attempted to fit eq 1 to the ϕ' angle data in Table II with all positive J 's on the M-LAB version of PROPHEX;²⁸ however, the fit (R) was never better than 0.922, which is a poor R factor. Several variations of positive and negative coupling constants were attempted. The procedure followed in these nonlinear least-squares fits is described below.

ϕ' Angle Fit. Since several low-angle data were available and one of the angles of **5B** was 2.2° , the initial fits of eq 1 used the data from **1B**, **2B**, **3B**, **4B**, and **6B** along with the constraint of eq 3, where $J_{0^\circ} = 19.5$ Hz. Using these fitted constants of A , B , and C , $J_{2.2^\circ}$ was computed to be 19.4 Hz. As J_{obsd} of **5B** is an average of $J_{2.2^\circ}$ and $J_{116.3^\circ}$, the latter coupling constant can be calculated (eq 4) assuming the sign of J_{obsd} is positive:

$$J_{116.3^\circ} = 2J_{\text{obsd}} - J_{2.2^\circ} = 2(28.2) - 19.4 = 37.0 \text{ Hz} \quad (4)$$

In addition, J_{180° can be computed for eq 2, from the $^3J_{\text{free}} = 27.1$ Hz for **9B**, and = 31.9 Hz for **10B** along with the J_{60° of 8.6 Hz for **6B**. If J_{free} and J_{60° are positive, then $J_{180^\circ} = 64.2$ and 78.5 Hz, but if J_{60° is negative then $J_{180^\circ} = 98.5$ and 112.9 Hz, respectively. Upon addition of $J_{116.3^\circ}$ and the two J_{180° to our data list, the fitted constants obtained for all positive J 's (eq 1: $A = 28.65$, $B = -22.43$, and $C = 13.27$ Hz) had an R factor of only 0.917. Allowing the coupling constants of **4B**, **6B**, and **2B** to be

(28) Bolt Beranek and Newman, Inc., Cambridge, Mass., and the Biotechnology Resources Program, Division of Research Resources, National Institutes of Health, with a terminal at the Anatomy Department of Georgetown University; Drs. A. Popper and G. Goeringer, principal investigators.

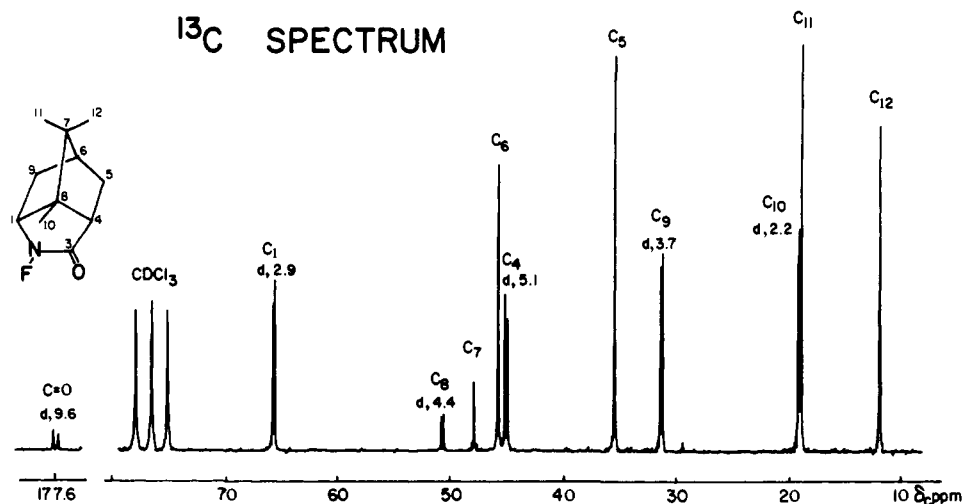


Figure 5. ^{13}C NMR proton decoupled spectrum of 2-fluoro-2-aza-7,7,8-trimethyltricyclo[4.2.1.0^{4,8}]nonan-3-one (**3B**) at 22.628 MHz in CDCl_3 downfield from internal $\text{Si}(\text{CH}_3)_4$. Note the ^{13}C - ^{19}F couplings (in Hz) for C_3 , C_1 , C_8 , C_4 , C_9 , and C_{10} .

negative, however, provided a quite good fit ($R = 0.990$) of the data as shown in eq 5 and plotted in Figure 6 (heavy curve).

$${}^3J_{\text{HF}} = 70.8 \cos^2 \phi' - 44.1 \cos \phi' - 7.2 \quad (5)$$

Integration²⁹ of eq 1 over 0–360° yields an expression for J_{free} shown in eq 6 that provides a simple check on the fitted constants.

$$J_{\text{free}} = A/2 + C \quad (6)$$

The calculated $J_{\text{free}} = 28.2$ Hz for the constants given in eq 5 is between the known J_{free} of compounds **9B** ($J = 27.1$ Hz) and **10B** ($J = 31.9$ Hz), while the “poor” constants for the all positive J 's predict $J_{\text{free}} = 27.6$ Hz, which is also very close. The excellent R factor fit for the inversion of sign curve, however, argues strongly for this solution. When further least-squares fits were made with the additional constraint of eq 6 = 27.1 and 31.9 Hz, the constants shown in eq 7 and 8, respectively, were obtained:

$${}^3J_{\text{HF}} = 72.1 \cos^2 \phi' - 43.7 \cos \phi' - 9.0 \quad (R = 0.990) \quad (7)$$

$${}^3J_{\text{HF}} = 66.6 \cos^2 \phi' - 45.7 \cos \phi' - 1.4 \quad (R = 0.987) \quad (8)$$

The fitted plots of ${}^3J_{\text{NF-CH}_a}$ vs. ϕ' for eq 5 (heavy curve), 7 (curve c), and 8 (curve b) are shown in Figure 6. Note that all three curves start at 19.5 Hz for J_{0° . This is the result of the constraint, $A + B + C = 19.5$, that was used to prevent the curves from floating because the **1A:1B** pair were the best known compounds we had available, as explained above. Until more data become available, the region described by these curves should be usable to determine ϕ' . A test case is provided by **7B**, which was not used in the Karplus equation fits. If all four angles are in rapid equilibrium and if the two twist chairs have equal populations, the calculated ${}^3J_{\text{av}} = -7.3$ Hz, which compares well with the observed coupling of 9.3 Hz. Changes of $<5^\circ$ for each of these angles would predict the observed coupling exactly.

ψ' Angle Fit. A similar fitting procedure was followed for the ψ' angle fitting to eq 9, except that only the data for compounds

$${}^4J_{\text{HF}} = A \cos^2 \psi' + B \cos \psi' + C \quad (9)$$

1B, **3B**, **4B**, **6B**, and the two possible J_{180° couplings (-21.3 or $+9.3$ and -27.0 and $+15.0$ Hz) calculated from ${}^4J_{\text{free}} = \pm 5.1$ Hz from **9B** and ± 7.0 Hz from **10B**, respectively, along with the $J_{60^\circ} = +3.00$ Hz from **6B** using eq 2. Again only the curve in which a double inversion of sign (negative to positive and back to negative at high angles) for ψ' gave reasonable R factors. Then $J_{2.6^\circ} = -5.47$ Hz and $J_{45^\circ} = +0.77$ Hz were calculated from the initial fitted parameters used in an equation similar to eq 4. These coupling constants plus the ${}^4J_{\text{obsd}}$ values were used to derive $J_{116.1^\circ}$ ($+0.59$ Hz) and J_{75° ($+4.15$ Hz) for **5B** and **2B**, respectively, and

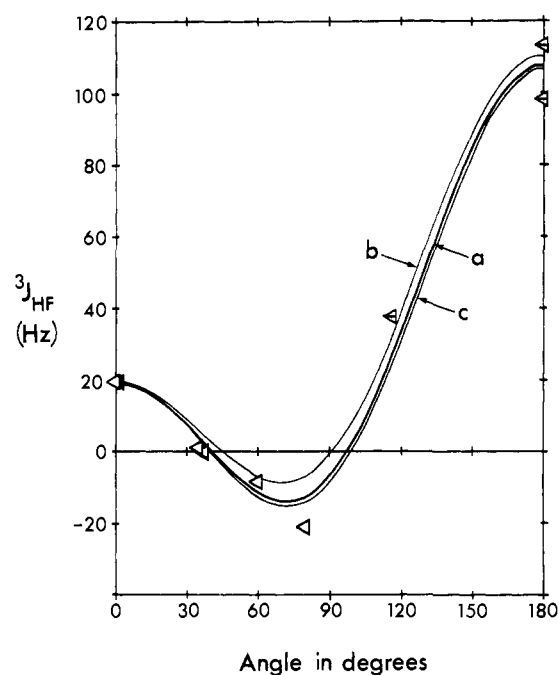


Figure 6. Karplus plots of the ${}^3J_{\text{NF-CH}_a}$ vs. the ϕ' angles derived from the data in Table II. The heavy line (curve a) is the best least-squares fit ($R = 0.990$) of eq 5. Curve b is a second fit (eq 8, $R = 0.987$) with an added constraint of eq 6 = 31.9 Hz (from **10B**), and curve c is another fit (eq 7, $R = 0.990$) with the same added constraint of eq 6 = 27.1 Hz (from **9B**). The open triangles are experimental data points; the closed triangle (2.2°) was computed from the initial least-squares fit to obtain the 116.3° point from J_{obsd} of compound **5B**. The crossed triangles at 180° were calculated from eq 2 and the observed ${}^3J_{\text{free}}$ of compounds **9B** and **10B**.

were added to the list for the final least-squares parameter fits. After applying the constraint of eq 3 = -5.9 Hz, the final fitted equation ($R = 0.983$) is

$${}^4J_{\text{HF}} = -19.5 \cos^2 \psi' + 8.8 \cos \psi' + 4.9 \quad (10)$$

and is shown in graphic form in Figure 7 as the heavy line (curve a). Equation 10 predicts $J_{\text{free}} = -4.9$ Hz compared to the experimental values of 5.1 to 7.0 Hz. It is, of course, possible to apply further constraints ($A/2 + C = -5.1$ and -7.0 Hz) to force an exact fit for J_{free} here because there are 10 points to fit. These gave eq 11 ($R = 0.983$, curve c in Figure 7) and 12 ($R = 0.965$,

$${}^4J_{\text{HF}} = -19.3 \cos^2 \psi' + 8.9 \cos \psi' + 4.6 \quad (11)$$

$${}^4J_{\text{HF}} = -17.3 \cos^2 \psi' + 9.8 \cos \psi' + 1.7 \quad (12)$$

(29) $J_{\text{free}} = \int_0^{360} (A \cos^2 \phi' + B \cos \phi' + C) d\phi' = A/2 + C$; in addition, several Karplus constant relations can be derived, such as eq 3; $J_{90^\circ} = C$ and $J_{180^\circ} = A - B + C$.

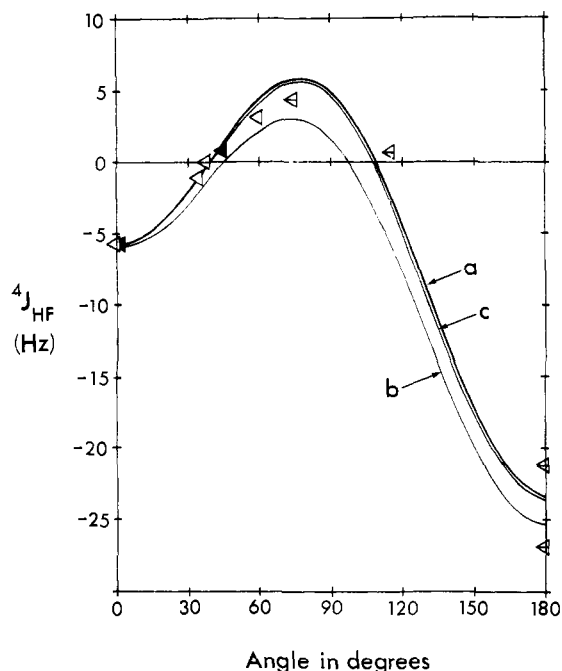


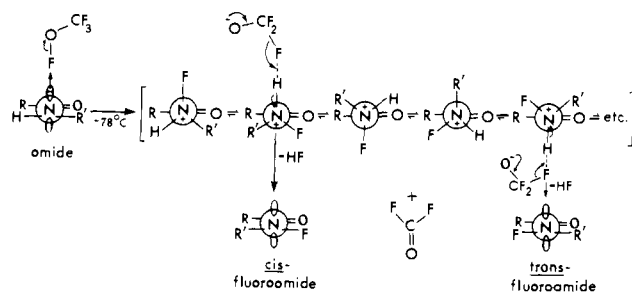
Figure 7. Karplus plots of the ${}^4J_{\text{NF-CO-CH}_2}$ vs. the ψ angles derived from the data in Table II. The heavy line (curve a) is the best least-squares fit ($R = 0.983$) of eq 10. Curve b is a second fit (eq 11, $R = 0.965$) with an added constraint of eq 6 = -7.0 Hz (from compound **10B**), and curve c is another fit (eq 12, $R = 0.983$) with the same added constraint (eq 6 = -5.1 Hz) from compound **9B**. The open triangles are experimental data points; the closed triangles (2.6 and 45°) were computed from the initial least-squares fit to obtain the 116.1 and 75° points (crossed triangles) from ${}^4J_{\text{obsd}}$ of compounds **5B** and **2B**, respectively. The remaining crossed triangles at 180° were calculated from eq 2 and ${}^4J_{\text{free}}$ of compounds **9B** and **10B**.

curve b) that provide a usable range for the ψ angle Karplus relation. A similar calculation of the ${}^4J_{\text{av}}$ for **7B** yields +3.3 Hz, which compares favorably with the ${}^4J_{\text{obsd}}$ of 4.7 Hz. In contrast to ${}^3J_{\text{av}}$, however, it is not possible to exactly predict ${}^4J_{\text{av}}$ with changes in the angles of $<5^\circ$. It is clear that more high-angle data are needed. We hope to obtain these data from cyclic peptides.

Concerning the Utility of These Karplus Relations. The utility of Figure 6 for the determination of the NF-C α H dihedral angle is very good, but its usefulness as a second determination of ϕ' remains to be proven. This will mainly depend on whether the exchange of the N-H to N-F bonds affects the conformation of a peptide. Initially, it would seem that the N-F bond should have the opposite polarity compared to an N-H bond. The chemistry of this fluorination, however, suggests a different conclusion. The monofluoroamide fluorinates faster than the original amide,¹ suggesting that the lone-pair electrons are more nucleophilic than the N-H lone-pair electrons. This could be true if a fluorine atom p orbital back-bonds into the π -electron system of the amide, an explanation that is used to account for the weak ortho,para directing character of fluorobenzene during electrophilic substitution. This process is also supported by the upfield shift of the carbonyl ${}^{13}\text{C}$ resonance in the N-F derivatives (cf. Table I). If back-bonding does occur, then the fluorine atom will carry a partial positive charge and so the N-F bond will have the same polarity as the normal N-H bonds in peptides. Consequently, there may not be a change in conformation. Work is in progress to resolve this problem and will be reported separately.

We also do not know if the relative signs of ${}^3J_{\text{HF}}$ and ${}^4J_{\text{HF}}$ start with opposite signs from those assumed here. Experiments are in progress to determine the signs of these couplings by several methods. One or more of these methods should be successful. Since both Karplus relations developed here undergo inversions of sign, it will be necessary eventually to have a routine method for determining the signs of the coupling constants. The signs of ${}^3J_{\text{HF}}$ in fluorocyclopropanes have been reported³⁰ to be positive

Scheme II



for 0° and 132°. While these are in agreement with our assignment, they were not determined experimentally. Finally one ${}^4J_{\text{HF}}$ has been reported to be negative,³¹ in agreement with the curve derived here.

There was concern early in this investigation that the fluorinated amide system might not be planar. Only an X-ray structure, which is being done and will be reported later, will give a final answer. But ${}^1\text{H}$ NMR temperature studies on **8B** and **9B** have been obtained that suggest there is a high barrier to rotation, which would occur if the *N*-fluoroamides are planar. **8A** was obtained as a 53:47 mixture of *cis*:*trans* amide isomers with ${}^3J_{\text{NH-C(O)H}} = 12.3$ and 2.0 Hz, respectively. Fluorination of this mixture gave only one isomer of **8B** (>99%) with ${}^3J_{\text{NF-C(O)H}} = 18.5$ Hz in close agreement with the reported³² 20.2-Hz coupling of the *cis*-amide isomer of *N*-fluoro-*N*-methylformamide (**11B**) vs. the smaller *trans*-amide coupling of 9.4 Hz. While Cantacuzene et al.³² observed an isomer dependence of **11B** with solvent changes, we did not, nor did any change occur from -60 to +120 °C in deuterated diglyme except that decomposition began at 110°, at which point **8B** slowly disappeared. This could be due to free rotation over the whole temperature range and simply a very small ΔG° difference between the two *cis*-*trans* rotamers, but it is more likely that no rotation occurs. This conclusion is reinforced by a similar temperature study on **9B**, which was obtained as a 95:5 mixture of *trans* to *cis* amides from the fluorination of **9A**. The ${}^3J_{\text{NF-CH}_3} = 27.1$ vs. 25.8 Hz, respectively, corresponds closely to the reported³² 26.3 vs. 24.8 Hz coupling constants for the *trans*:*cis* amide isomers of **11B**. Again no change occurred in the ${}^1\text{H}$ spectra from -60 to +35 °C in CDCl_3 and 35 to 140 °C in d_5 -nitrobenzene except that decomposition began at 134 °C. We believe these results support a high barrier to rotation in both **8B** and **9B**.

The above results suggest that the isomeric ratio obtained during fluorination is permanent and may be the result of the rotamer stability of the *N*-tetrahedral amidonium ion intermediate obtained from the initial transfer of the fluorine atom from CF_3OF to the amide as shown in Scheme II. In the *cis*-amide compounds (**1A** to **7A**), the intermediate cannot rotate and must form the *cis* fluoroamides (**1B** to **7B**), but rotamer equilibria can be involved in the open-chain intermediates obtained from **8A** and **9A**. The relative stabilities of these latter intermediates then dominate the product ratios and not necessarily the relative isomer stabilities or the height of the energy barrier between the isomers. The *N*-*tert*-butyl group of **8A** is bulkier than the long chain of **9A** and therefore produces a larger amount of the least hindered rotamer that leads to a higher proportion (>99%) of the *cis*-**8B** while **9A** yields 95% *trans*- and 5% *cis*-**9B**.

Acknowledgment. We wish to thank the National Science Foundation for partial funds for our Bruker WH-90 FT-NMR instrument (Grant No. CHE 76-05887) and Dr. William Egan of the Bureau of Biologics, Food and Drug Administration, Washington, DC, for the use of his Bruker WN-300 FT-NMR instrument and for several interesting discussions. We appreciate the helpful discussions of Professors A. A. Bothner-by of Car-

(30) (a) Williamson, K. L.; Mosser, S.; Stedman, D. E. *J. Am. Chem. Soc.* **1971**, *93*, 7208. (b) Williamson, K. L.; Hsu, Y-F. L.; Hall, F. H.; Swager, S.; Coulter, M. *Ibid.* **1968**, *90*, 6717.

(31) Schaefer, T.; Marat, K. *Org. Magn. Reson.* **1981**, *15*, 294.

(32) Cantacuzene, J.; Leroy, J.; Jantzen, R.; Dudragne, F. *J. Am. Chem. Soc.* **1972**, *94*, 7924.

negie-Mellon University and Lila Gierasch of the University of Delaware. We thank Mr. Michael M. Kornbluth for his assistance in the data analysis and management, which was mainly performed using the PROPHET computer network developed and supported by the Division of Research Resources, NIH. We also appreciate the diligent efforts of Mr. William H. Craig for maintaining our WH-90 and for his innovative electronic wizardry in building the high-power homodecoupler described herein. Finally, we thank

Miss Alice L. Reid for her data on compound **10B**.²³

Registry No. **1A**, 3306-69-2; **1B**, 88842-37-9; **2A**, 88842-36-8; **2B**, 88842-38-0; **3A**, 37488-26-9; **3B**, 88842-39-1; **4A**, 25772-44-5; **4B**, 88842-40-4; **5A**, 105-60-2; **5B**, 23649-75-4; **6A**, 616-45-5; **6B**, 23649-65-2; **7A**, 675-20-7; **7B**, 23649-68-5; **8A**, 2425-74-3; **8B**, 88842-41-5; **9A**, 20198-92-9; **9B**, 52072-73-8; **10A**, 1906-82-7; **10B**, 88842-42-6; camphene, 79-92-5; chlorosulfonyl isocyanate, 1189-71-5; α -pinene, 80-56-8; cycloheptatriene, 544-25-2; CF₃OF, 373-91-1.

Molecular Orbital Study on the Hydrolysis of Ketene by Water Dimer: β -Carbon vs. Oxygen Protonation?

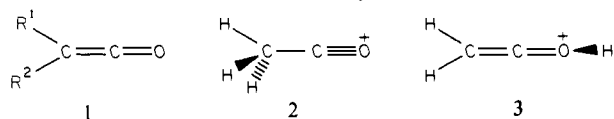
Minh Tho Nguyen[†] and A. F. Hegarty*[‡]

Contribution from the Department of Chemistry, University of Leuven, B-8030-Heverlee, Belgium, and Department of Chemistry, University College Belfield, Dublin 4, Ireland.

Received May 13, 1983

Abstract: The detailed reaction pathway for the hydration of ketene (CH₂=C=O) by water dimer has been investigated by ab initio methods using STO-3G and 4-31G basis sets. Two transition states for the reaction have been compared (using the gradient method to determine saddle points on the energy surface) involving addition of water across the C=C and C=O bonds. The latter process (to yield a ketene hydrate CH₂=C(OH)₂ initially) is markedly favored (activation barrier 13 kcal mol⁻¹), compared to direct formation of acetic acid (24 kcal mol⁻¹, also in 4-31G). This contrasts with preequilibrium proton transfer to the carbon of the ketene, which gives a more stable species (CH₃CO⁺) than does proton transfer to oxygen (to give CH₂COH⁺). These findings are compared with experimental results and the intermediacy of reactive ketene hydrates and cyclic mechanisms commented on.

Ketenes (**1**), as members of the cumulene family, undergo a wide range of additions with nucleophilic reagents and cycloadditions to unsaturated substrates; they also serve as intermediates



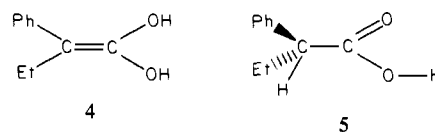
for acylation reactions.¹ It is well-known that in a strongly acidic mixture, the rapid protonation of ketenes occurs at the terminal carbon atom (C_β) rather than at the oxygen atom.² The energy difference between the C_β-protonated (**2**) and oxygen-protonated (**3**) isomers was calculated to be 37 kcal/mol at SCF level with double- ζ basis set³ in favor of C_β-protonated ketene **2**.

In the spontaneous reaction of ketenes with nucleophilic reagents such as alcohols, amines, and carboxylic acids, nucleophilic attack at the C_α atom was generally accompanied by a proton transfer to the C_β atom.⁴ In the same way, the hydrolysis of various ketenes classically leads to the formation of carboxylic acids.⁵ These additions were assumed from kinetic studies to occur via cyclic transition states that involve the C=C bond of ketenes.⁶

Bothe and co-workers⁷ recently reported an experimental study of the rate and mechanism of hydration of the unsubstituted ketene (CH₂=C=O). In aqueous solution (pH 4.4-9.85), the observed rate constants for hydrolysis were shown to be independent of pH but approximately proportional to the water concentration. A solvent kinetic isotope effect of $k_{H_2O}/k_{D_2O} = 1.9$ has been measured. These authors also reported an activation enthalpy of 10.3 kcal/mol and an activation entropy of -16 eu. Acetic acid as its dissociated form is observed as product. It is concluded that the water is acting as nucleophilic reagent rather than the proton (H⁺ or H₃O⁺) donor in the first step of the hydrolysis. However, the question remains unanswered as to whether the acetic acid was

produced directly from this first step or only in a subsequent step, that is, whether the hydrolysis has occurred by C_β protonation or by oxygen protonation.

More recently, we have carried out the hydration of phenylethylketene in an acetonitrile/water mixture with 1-5% of water. From our kinetic measurements⁸ we cannot rule out the participation of the 1,1-ethylenediol **4** as an intermediate in the hydrolysis of phenylethylketene (the final product is the substituted acetic acid **5**). In solution, the transformation of enol **4** to ketone **5** should be a fast process.



We have also observed a strongly negative activation entropy of -50 eu for the formation of **5**, which is much larger than the value of -16 eu previously reported for CH₂CO.⁷ However, this entropy value, which suggests a highly ordered activated complex, appears to be consistent with the observation of Satchell et al.^{5,6} According to these authors, the spontaneous hydration of ketenes with water is autocatalytic, the cyclic transition states containing, besides the ketene molecule, two water molecules. These latter react as a dimer rather than two monomers. Moreover, there is

(1) For leading references see: "The Chemistry of Ketenes, Allenes and Related compounds"; Patai, S., Ed.; Wiley: New York, 1980; Parts I and II.

(2) Olah, G. A.; Dunne, K.; Ho, Y. K.; Szilgyi, P. *J. Am. Chem. Soc.* **1972**, *94*, 4200.

(3) Yakorny, D. R.; Schaefer, H. F., III *J. Chem. Phys.* **1975**, *63*, 4317.

(4) Briody, J. M.; Lillford, P. J.; Satchell, D. P. N. *J. Chem. Soc. B* **1968**, 885.

(5) Lillford, P. J.; Satchell, D. P. N. *J. Chem. Soc. B* **1968**, 889.

(6) Satchell, D. P. N.; Satchell, R. S. *Chem. Soc. Rev.* **1975**, *4*, 231.

(7) Bothe, E.; Dessouki, A. M.; Schulte-Frohlinde, D. *J. Phys. Chem.* **1980**, *84*, 3270.

(8) Hegarty, A. F.; O'Connell, J., unpublished results.

[†]University of Leuven.

[‡]University College Dublin.